BJRS

BRAZILIAN JOURNAL
OF
RADIATION SCIENCES
11-04 (2023) | 01-14 | e2342

Evaluation of radiation damage exposure for low alloy steel in J-9 irradiation channel of Argonauta reactor

Ogihara[a], J.T.; Silva[b], P.B.R.; Araújo-Moreira[a], F.M.

[a] *Programa de Pós Graduação em Engenharia Nuclear/IME/Seção de Engenharia Nuclear, 22290-270, Rio de Janeiro, RJ, Brazil*

[b] *Diretoria de Desenvolvimento Nuclear da Marinha, 05508-000, São Paulo, SP, Brazil*

jonnathan.toshio@ime.eb.br , *benevides@marinha.mil.br*, *fernando.manuel@ime.eb.br*

ABSTRACT

The operation of nuclear facilities must satisfy the nuclear safety requirements. An analysis of the components of these facilities focuses on the structural materials. In this scenario, several types of alloys are employed in their construction. The nuclear fuel burn-up will result in damage caused by ionizing radiation. Due to continuous operation, radiation damage will build up and may result in the manifestation of macroscopic radiation effects. Such effects may change the mechanical, physical and chemical properties of structural alloys. Thus, it is verified the importance of the material behavior predictability to avoid reduction in performance or failure in these types of facilities. In order to study these effects, it's necessary to calculate the displacement per atom (dpa) in the material. This calculation was estimated for the reactor Argonauta's irradiation channel J-9 for low alloy steel. An ideal situation with a harder neutron spectrum was calculated to analyze the results. The dpa rate calculated in that facility was attributed to the low neutron energy fluence.

Keywords: **nuclear safety, materials, radiation damage, radiation effects, displacement per atom**

ISSN: 2319-0612
DOI: https://doi.org/10.15392/2319-0612.2023.2342
Submitted: 2023-09-12
Accepted: 2023-11-06

1. INTRODUCTION

A nuclear facility is defined by Comissão Nuclear de Energia Nuclear (CNEN)[1] [1] as an authorized facility in which nuclear material is produced, processed, reprocessed, utilized, handled or stored in significant quantities. Nuclear reactors and power plants, where nuclear fuel is used to produce thermal and electrical energy for industrial purposes are included in this definition. The design, operation and control of a nuclear reactor are analyzed, regardless of its purpose (power, research, propulsion). An important parameter to be studied is the variety of structural materials applied in its components [2], as shown in Figure 1.

Figure 1: *Schematic of a pressurized water reactor (PWR) and its constituents materials.*

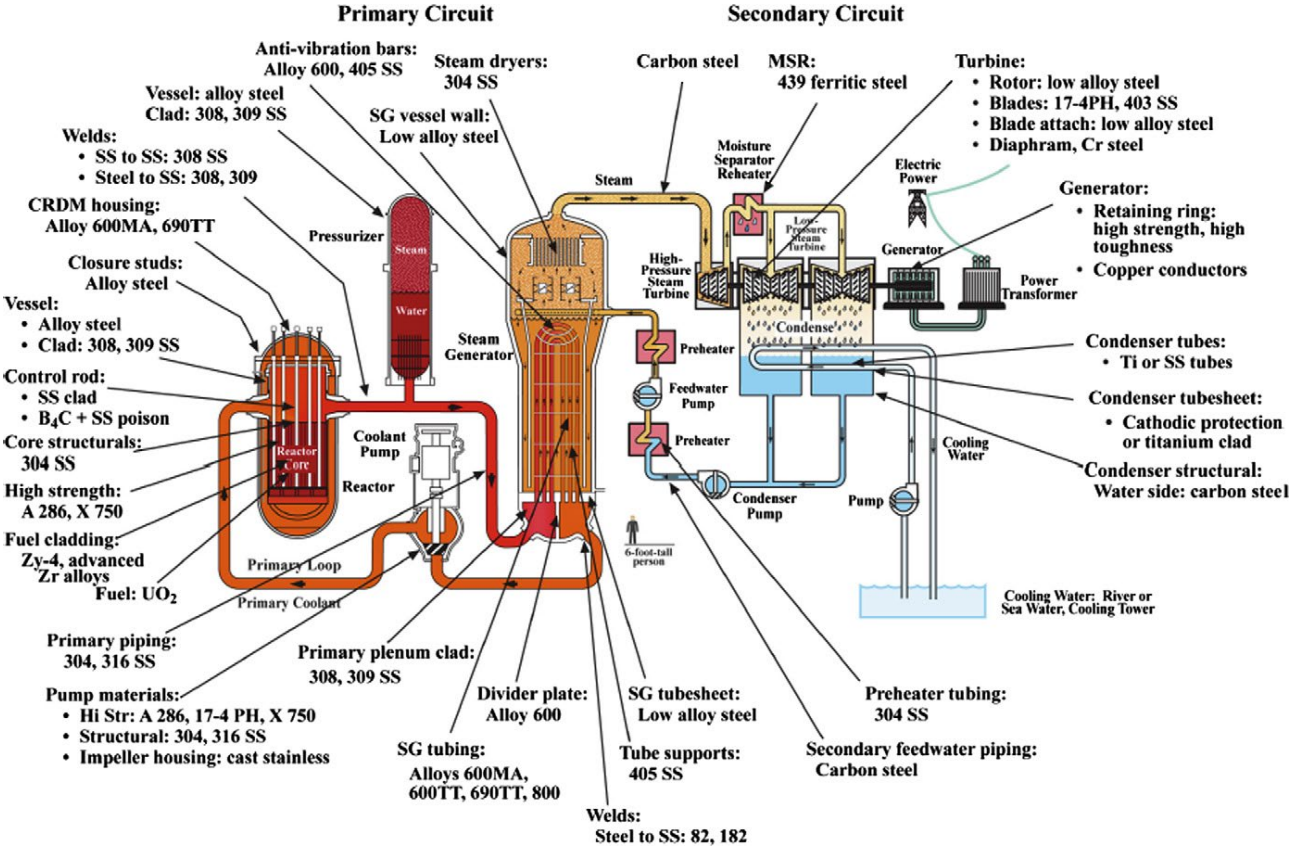

Source: Zinkle and Was (2013) [3]

[1] CNEN, federal autarchy, created by Brazilian Law n° 4.118/1962, has the legal competence of formulate specific guidelines for radiological protection and nuclear safety, cientific and technology works, industrials and other nuclear applications, according to item II, act. 2°, Brazilian Law n° 7.781/1989.

These materials must have characteristics that guarantee their reliable performance within the design criteria during the operation of a nuclear reactor [2], i.e., they must be able to fulfill the requirements of nuclear safety, defined by CNEN [1] as the achievement of operational conditions, prevention and control of accidents and appropriate mitigation of the consequences of accidents, resulting in the protection of individual and the environment against radiation risks.

These materials are inserted in an extremely aggressive environment, especially in the reactor core, where high temperatures, high stresses, corrosion and radiation damaged caused by high-energy particles released during the fission reaction chain reactions of nuclear fuel are particularly important. The materials are exposed to continuous degradation of their properties throughout the operating life of a nuclear reactor in this scenario. The dominant form of degradation will depend on the type of material and the different environmental circumstances in which the component will operate [4].

In the field of metals, the main radiation damage is caused by high-energy radiation, mainly neutrons and fission by-products [3]. According to Murty and Charit [5], other types of radiation do not have the necessary energy or are not produced in sufficient numerical density to cause major radiation damage.

Radiation damage is defined as the microscopic defects produced by irradiation. The interaction of radiation with the material can produce a variety of defects and the main one is the Frenkel pair, a vacancy-autointerstitial pair. The accumulation of the different defects results in macroscopic changes in the physical, chemical and mechanical properties of the material, a phenomenon defined as radiation effects [5].

According to displacement theory, the incident particle must have enough energy to displace an atom from its position in the crystal lattice and transfer part of its energy. This first event defines the creation of a primary knock-on atom (PKA). In turn, the PKA, provided with kinetic energy transferred by the radiation, will interact with other atoms in the crystal lattice, giving rise to various defects, interactions and secondary, tertiary, and so on, knock-on atoms. This collection of defects created by the PKA is called a displacement cascade. The event will end when the PKA occupies its final position in the crystal in the form of an interstitial and generates an emptied region as a result of these interactions [6].

Various radiation effects can occur simultaneously depending on the temperature range in which the material is irradiated. For the purposes of this work, mention should be made of low-

temperature radiation hardening and embrittlement. This effect arises from the increase in defects in the metal's crystal lattice. These microstructural defects provide barriers to the plastic deformation of the material when stress is applied. The increase in yield strength could be beneficial, but is usually accompanied by a decrease of ductility and toughness, which act in favor of the safety of a nuclear facility [7]. These properties changes can be observed in Figure 2, which shows the engineering stress-strain curves for high-purity polycrystalline copper and nickel and commercial-purity 316 stainless steel (316 SS) irradiated with neutrons at the indicated doses (dpa) [8].

Figure 2: *Engineering stress-strain curves of materials irradiated at room temperature*

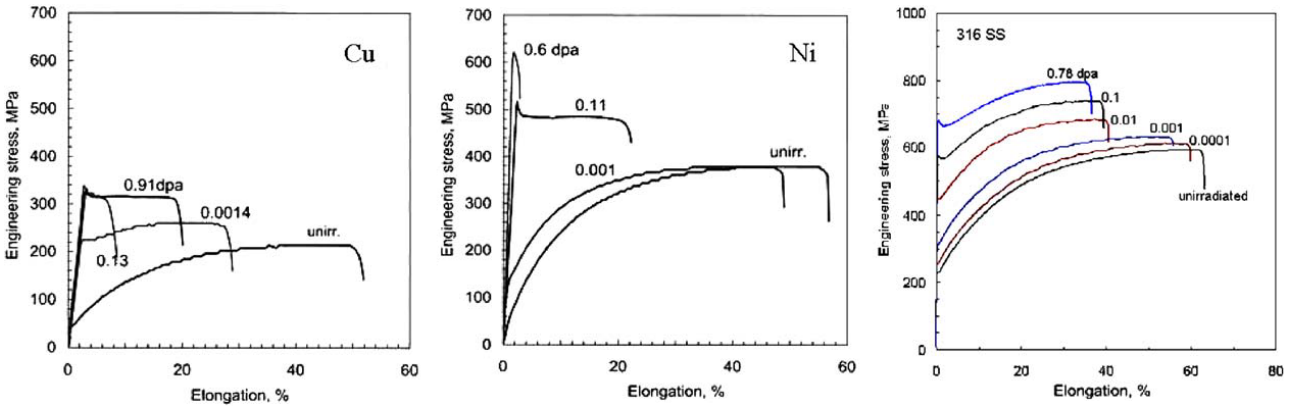

Source: Hashimoto, Byun and Farrell (2006) [8]

Another result of this effect is the increase of ductile-brittle transition temperature. This variation must be known in order to guarantee the nuclear safety of a facility. During the routine cold shutdown of a reactor for reloading, a wide thermal variation occurs. This situation can lead to temperatures at which the material will exhibit brittle behavior. [3].

A practical example of radiation effects is presented in Figure 3. Brittle fracture was observed in the austenitic stainless steel reflector assembly ducts of fast research reactor BOR-60 (Russia). The failure occurred during scheduled maintenance involving the removal of these ducts and was associated with high stress in the procedure and irradiation effects [7]. Thus, it is observed the relevance of the study on this subject, in order to avoid reduction in performance or failure.

Figure 3: *Brittle fracture in BOR-60's reflector assembly ducts*

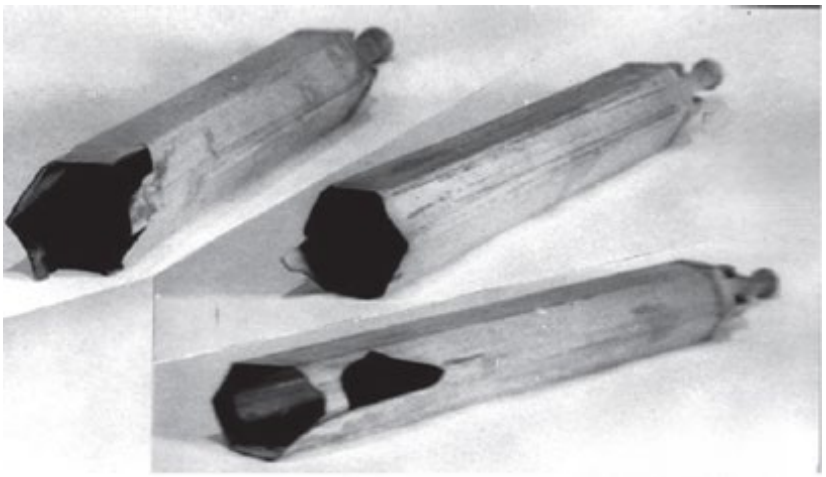

Source: Zinkle, Tanigawa and Wirth (2019) [7]

1.1. Radiation Damage Evaluation

As presented, it can be verified that one of the main impact factors for the development of these effects is associated with the amount of radiation received by the material. One of the metrics adopted to evaluate radiation damage has been defined as the displacement per atom (dpa) [5]. This unit of radiation exposure measures the average amount that an atom is displaced from its position in the crystal lattice [9].

By disregarding the different spectra associated with the incident flow, analysis of the damage caused based on fluence alone can provide values with low correlation for the same type of material. This situation is observed in Figure 4, which shows the results obtained for changes in yield strength for 316 SS alloy specimens irradiated at three different facilities: Los Alamos Spallation Radiation Effects Facility (LASREF) has a flux with a broad spectrum of high-energy neutrons obtained from a Be(d,n) beryllium source; Rotating Target Neutron Source-II (RTNS-II) provides a beam of 14 MeV monoenergetic neutrons and Omega West Reactor (OWR) provides a spectrum typical of light water reactors. When the results are presented as a function of dpa, it is possible to verify a tendency for increasing hardness of the irradiated material [10].

Figure 4: *Comparison of the yield strength of 316 SS alloy irradiated at three different facilities presented as a function of neutron fluence and dpa*

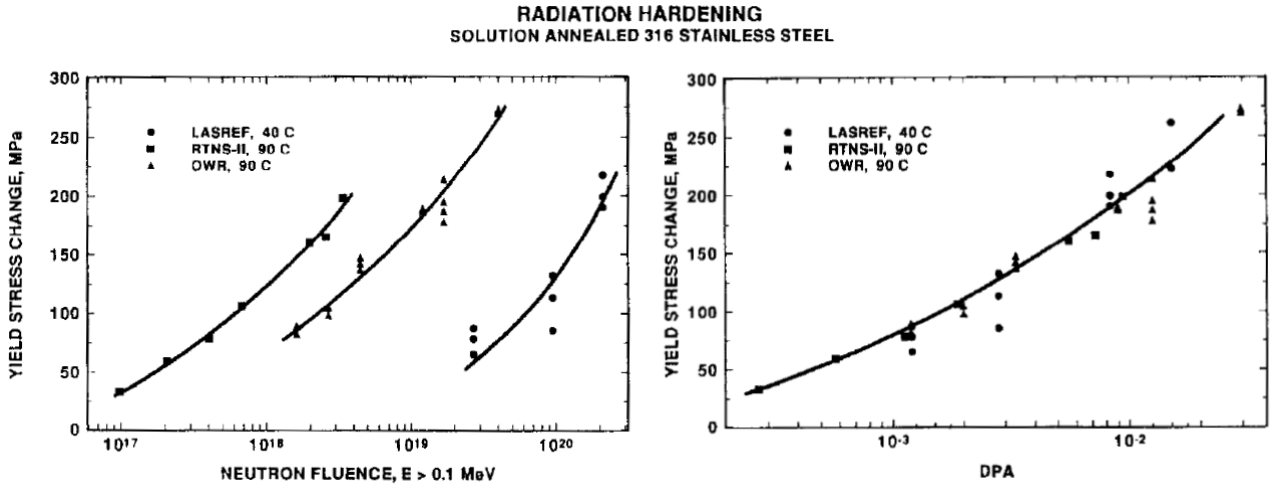

Source: Greenwood (1994) [10]

The terms of reaction rate equation can be written in the form of Equation 1. Displacement reaction rate R_D will be equivalent to the number of atoms displaced per unit volume in a given time, $\check{E}$ and $\hat{E}$ correspond to the minimum and maximum energy of the incident particle, $\phi(E_i)$ is the energy-dependent incident particle flux and $\sigma_D(E_i)$ is the energy-dependent displacement cross-section of the incident particle [6]. Rearranging the terms, the dpa rate is defined by Equation 2 [5].

$$R_D = N \int_{\check{E}}^{\hat{E}} \phi(E_i)\sigma_D(E_i)dE_i \tag{1}$$

$$\frac{dpa}{t} = \int_{\check{E}}^{\hat{E}} \phi(E_i)\sigma_D(E_i)dE_i \tag{2}$$

Different ways can be used to calculate the displacement cross-sections. In order to present the typical behavior of this variable, Figure 5 shows a comparison between the displacement cross-sections obtained for iron calculated using two different models, arc-dpa and the NRT model. The binding energy of the atom to the crystal lattice corresponds to the threshold energy [5], adopted as *40 eV* for iron [11].

Figure 5: *Displacement cross-section for iron obtained from the NRT and arc-dpa*

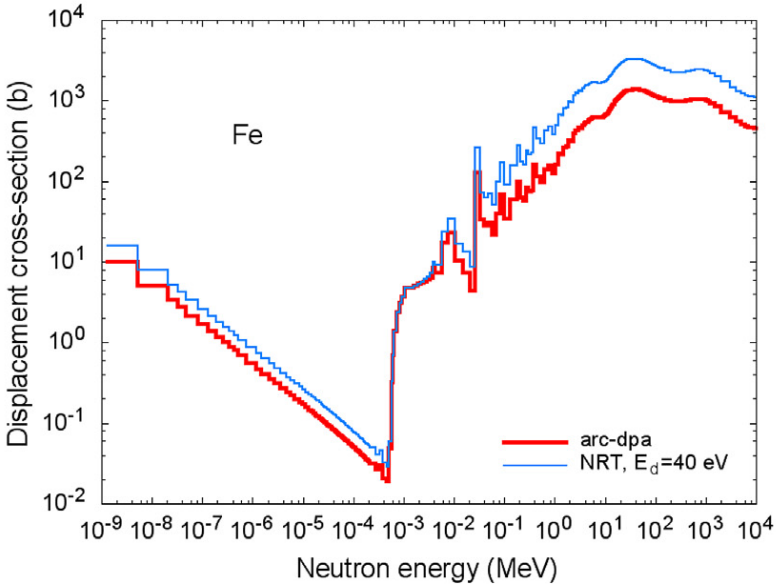

Source: Konoboyev, Fischer and Simakov (2018) [11]

Considering the concepts above, this article aims to present the dpa calculations for low alloy steel specimens inserted into the main irradiation channel (J-9) of the Argonauta reactor. The material was selected due to its frequent application in power plants, as can be identified in Figure 1, with particular emphasis on its use in reactor pressure vessels [12]. The nuclear irradiation facility to be investigated was selected considering that no studies were verified in this area.

2. MATERIALS AND METHODS

2.1. Argonauta Reactor

The Argonauta reactor is a nuclear research facility in Ilha do Fundão, Rio de Janeiro. In its current configuration, the reactor can reach a peak power of 1 kW for one hour of operation and 500 W for continuous operation. Its core is arranged in two aluminum cylinders positioned concentrically to form a ring, named fuel region. The distribution in this region consists of 24 positions for arranging the fuel elements, with the current configuration allocating only one ring segment, as can be seen in Figure 6. The fuel elements are made up of plates consisting of a mixture of aluminum and triuranium octoxide (U_3O_8), enriched in 19.91 % U-235. The reactor has thirteen

irradiation channels, the main one is J-9 which reaches the external tank at half height (highest neutron flux) [13-15].

Figure 6: *Layout of the core and the J-9 irradiation channel of the Argonauta reactor*

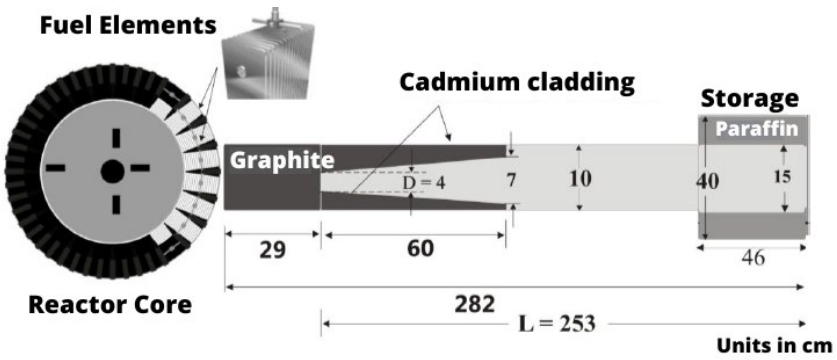

Source: Souza (2012) [13]

2.2. Displacement per Atom Calculation

The ASTM-E693-23 [9] standard can be used to define the displacement cross-section. It is statement that the values obtained for iron are an adequate approximation for calculating displacements for steels, almost entirely made up of this element (95 to 100%), in radiation fields where secondary damage processes are not important. In this sense, the use of this standard is suitable for the correlation of parameters for neutron irradiation, such as low alloy steel within this range of composition. In accordance with this standard, the discretized displacement cross-section values $\sigma_D\ (E_n)$ for natural iron for neutrons with energy E_n available were adopted, for a total of $n = 139$ data sets between $0.000105 \leq E_n \leq 0.12\ eV$.

In order to verify the possibility of developing a study with material irradiation in the Argonauta reactor, for the J-9 channel, an overrated flux of $10E+10\ n.cm^{-2}.s^{-1}$ was considered, applying the Maxwell-Boltzmann distribution function, according to references [13-15]. This function was calculated using the normalized formula in Equation 3 [16], where $m = 1.67494E27\ kg$, $k = 8.617E\text{-}5\ eV/K$ and $T = 293K$.

$$f_{MB}(E_n) = \frac{2\pi}{(2\pi kT)^{3/2}} {E_n}^{1/2} e^{-E_n/kT} \tag{3}$$

Energy-dependent flux $\phi(E_n)$ was calculated using Equation 4, where $\phi = 10^{10}\ n.cm^{-2}.s^{-1}$.

$$\phi(E_n) = \phi\, f_{MB}(E_n) \tag{4}$$

The energy range ΔE_n was calculated using Equation 5, where for $n = 140$, $E_{140} = 0{,}1275\ eV$.

$$\Delta E_n = E_{n+1} - E_n \tag{5}$$

The dpa rate was calculated using Equation 6.

$$\frac{dpa}{t} = \sum_{i=1}^{n} \sigma_D(E_n)\, \phi(E_n) \Delta E_n \tag{6}$$

For a more comprehensive analysis of the results, calculations were also performed applying the Watt fission spectrum, an empirical formula which describes the distribution of prompt neutrons induced by the thermal fission of U-235 [17]. It is assumed that this would be the ideal condition for irradiation with the hardest spectrum emerging from the reactor core. The same calculation methodology was applied, adopting a total of $n=136$ data sets between $0.1 \leq E_n \leq 10.0\ MeV$, $E_{137} = 10{,}1\ MeV$ for Equation 5 and replacing Equation 3 with Equation 7 (E in unit of *MeV*).

$$\chi = 0.453 e^{-1.036E} sinh\sqrt{2.29E} \tag{7}$$

3. RESULTS AND DISCUSSION

In order to present the calculations performed and an analysis of the results for J-9 channel, the discretized values were grouped together as can be seen in Table 1. The behavior of the displacement cross-section and the energy-dependent flux as function of the incident neutron energy in the range covered by calculation can be better visualized in the graphs in Figure 7.

Table 1: Neutron flux and dpa rate calculated for J-9 channel

N	Neutron energy	Neutron flux		Dpa	
	(eV)	(n.cm^{-2}.s^{-1})	(%)	(s^{-1})	(%)
1-35	0.00011-0.00063	2.89E+07	0	2.49E-15	2
36-70	0.00066-0.00380	3.96E+08	4	1.39E-14	12
71-105	0.00400-0.02200	3.47E+09	35	5.27E-14	45
106-139	0.02300-0.12000	6.16E+09	61	4.80E-14	41
	Total	**≈1.00E+10**	**100**	**1.17E-13**	**100**

Figure 7: *Displacement cross-section and energy-dependent neutron flux per neutron energy for J-9 channel*

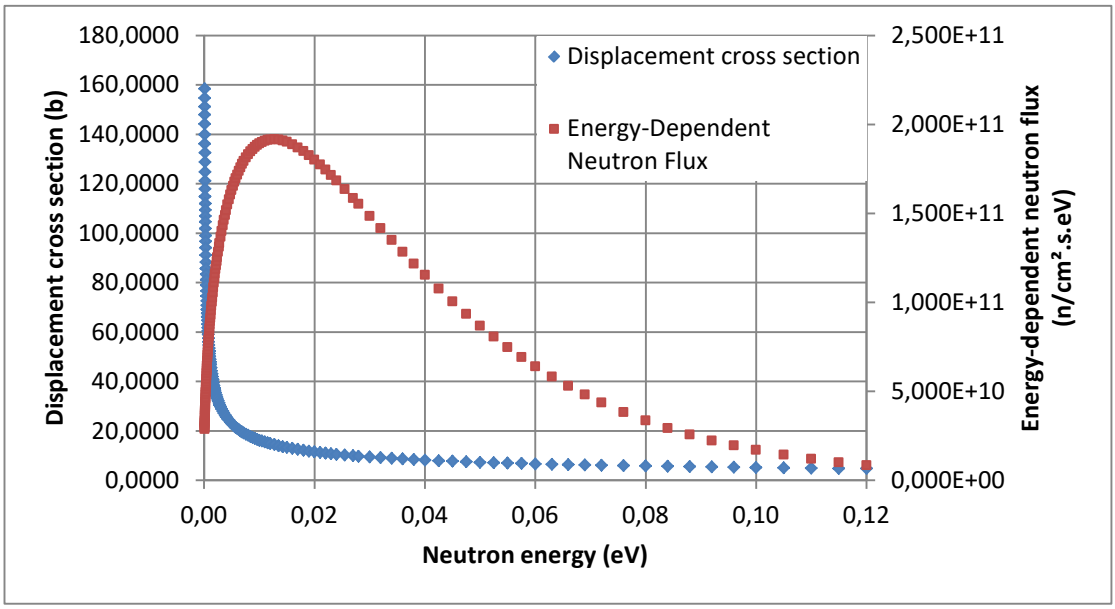

Therefore, the dpa rate calculated under the conditions presented was *1.17E-13* s^{-1} or *4.21E-10* h^{-1}. Considering the minimum values presented in the references [8,10], in the order of *0.0001 dpa*, it can be verified that the irradiation time required to obtain appreciable changes produced by the effects of radiation in the context of low-temperature radiation hardening and embrittlement would be far too long. Assuming an irradiation routine of 6 hours a day, it would take around 400,000 days to produce *0.0001 dpa* in the material.

Analyzing the groups formed from the energy ranges of the incident neutron, it can be seen that the neutron flux for n between 1-35 is insignificant but is still capable of producing a not so insignificant dpa rate. This is due to the higher values of the displacement cross-section resulting from radiative capture reactions. This type of interaction is capable of displacing atoms in the crystal lattice as a function of the resulting recoil energy in the nucleus due to the conservation of momentum when the γ ray is emitted [6]. As the neutron energy increases and the probability of interaction by (n,γ) decreases in the ratio *1/v* or $1/E^{1/2}$ [17], the flux becomes more relevant in accounting for the dpa rate, as observed in the n 71-105 and 106-139 groups.

In addition, the dpa rate could be even lower if more realistic neutron flux values were used for the J-9 channel. Furthermore, the method employed by the ASTM-E693-23 standard is based on the

NRT model, which provides slightly higher values of the displacement cross-section when compared to the arc-dpa model (Figure 5).

The discretized values for Watt spectrum calculation are also presented in groups in Table 2. The behavior of the displacement cross-section and the energy-dependent flux as function of the incident neutron energy in the range covered by calculation are presented in the graphs in Figure 8.

Table 2: Neutron flux and dpa rate calculated with Watt spectrum

N	Neutron energy	Neutron flux		Dpa	
	(MeV)	($n.cm^{-2}.s^{-1}$)	(%)	(s^{-1})	(%)
1-35	0.10-0.60	1.64E+09	16	4.69E-13	5
36-70	0.63-3.40	6.86E+09	69	5.42E-12	65
71-105	3.50-6.90	1.42E+09	14	2.23E-12	27
106-136	7.00-10.00	1.08E+08	1	2.17E-13	3
Total		**≈1.00E+10**	**100**	**8.34E-12**	**100**

Figure 8: *Displacement cross-section and energy-dependent neutron flux per neutron energy for Watt spectrum*

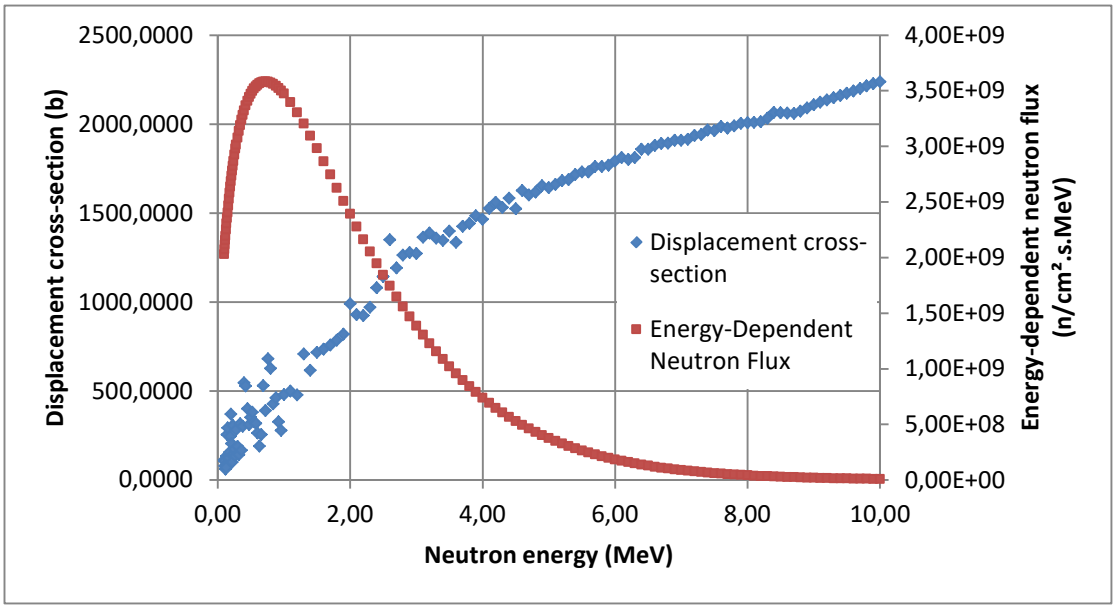

It can be observed that the results agree with the references [5,6]. A higher dpa rate is expected to the irradiated material when a harder spectrum (*E>0,1 MeV*) is applied due to the production of

PKA with higher imparted energy and hence the production of a wider dislocation cascade. This behavior is observed in the groups shown in Table 2, in which the most energetic neutron group is capable of producing about three times more damage with an equivalent flux.

It is worth mentioning that other nuclear reactions are becoming more likely to occur, such as inelastic scattering (n,n') and neutron production (n,2n), with incident neutrons of energy exceeding 1.0 MeV and 8.0 MeV, respectively [6]. The contribution of these reactions is evident in Figure 8 in the higher values of the displacement cross-section for adopted Watt spectrum range.

Although a more severe situation is assumed by assuming the Watt spectrum to the neutron flux, it can be observed that the irradiation time required under the conditions presented above for appreciable changes in the order of 0.0001 dpa would still be more than 555 days. Therefore, it is possible to state that the main limitation for irradiation damage with the Argonauta reactor is its low neutron flux. As expected, the estimated dpa level is much lower than that used by Hashimoto, Byun and Farrell [8], who irradiated their specimens in the range *1.1E+17* to *6.3E+20 n.cm*$^{-2}$ with neutrons of *E > 0.1 MeV*, corresponding to levels between *0.0001* and *0.92 dpa.*

4. CONCLUSIONS

This article presents the importance of studying the behavior of structural materials exposed to ionizing radiation in nuclear facilities. Concepts related to the radiation damage and effects on alloys used in nuclear facilities were also explained.

In this sense, the dpa metric used to compare irradiated specimens was presented and its rate was calculated for the main irradiation channel (J-9) of the Argonauta reactor, based on the ASTM-E693-23 standard. The values were analyzed and found to be consistent with the references. An ideal condition that would provide the most severe situation for applying radiation damage was also calculated assuming the Watt spectrum.

More realistic values to neutron flux and spectrum can be applied in further calculation to improve the results, although it was found that the application of the Argonauta reactor in its current configuration for irradiation damage to specimens is limited to its low neutron flux. In addition, other calculation methodologies and nuclear data can be used to estimate the dpa rate.

ACKNOWLEDGMENT

We would like to thank Marinha do Brasil, especially Diretoria de Desenvolvimento Nuclear da Marinha (DDNM), Instituto Militar de Engenharia (IME) and Instituto de Engenharia Nuclear (IEN) for providing support to our research.

REFERENCES

[1] COMISSÃO NACIONAL DE ENERGIA NUCLEAR. **CNEN: Glossário do setor nuclear e radiológico brasileiro.** Rio de Janeiro, 2020. 50 p.

[2] BUSBY, J. T. Overview of structural material in water-cooled fission reactor. In:_____. **Structural Alloys for Nuclear Energy Applications.** Amsterdan: Elsevier, 2019. p. 1–21.

[3] ZINKLE, S. J.; WAS, G. S. Materials challenge in nuclear energy. **Acta Materialia**, v. 61, n. 3, p. 735–758, 2013.

[4] ALLEN, T.; BUSBY, J.; MEYER, M.; PETTI, D. Materials challenge for nuclear systems. **Materials Today**, v. 13, n. 12, p. 14–23, 2010.

[5] MURTY, K. L.; CHARIT, I. **An Introduction to Nuclear Materials - Fundamentals and Applications.** 1. ed. Weinheim: Wiley-VCH, 2013. 382 p.

[6] WAS, G. S. **Fundamentals of Radiation Materials Science - Metals and Alloys.** 1. ed. Heidelberg: Springer Berlin, 2007. 827 p.

[7] ZINKLE, S. J.; TANIGAWA, H.; WIRTH, B. D. Radiation and thermomechanical degradation effects in reactor structural alloys. In:_____. **Structural Alloys for Nuclear Energy Applications.** Amsterdam: Elsevier, 2019. p. 163–210.

[8] HASHIMOTO, N.; BYUN, T. S.; FARRELL, K. Microstructural analysis of deformation in neutron-irradiated fcc materials. **Journal of Nuclear Materials**, v. 351, n. 1-3, p. 295–302, 2006.

[9] AMERCIAN ASSOCIATY FOR TESTING AND MATERIALS. **ASTM E693-23**: Standard practice for characterizing neutron exposures in iron and low alloy steels in terms of displacement per atom (dpa). West Conshohocken, 2023. 8 p.

[10] GREENWOOD, L. R. Neutron interactions and atomic recoil spectra. **Journal of Nuclear Materials**, v. 215, p. 29–44, 1994.

[11] KONOBEYEV, A. Yu; FISCHER, U.; SIMAKOV, S. P. Atomic displacement cross-sections for neutron irradiation of materials from Be to Bi using the arc-dpa model. **Nuclear Engineering and Design**, v. 51, n. 1, p. 170–175, 2018.

[12] WILLIAMS, T.; NANSTAD, R. Low-alloy steels. In:_____. **Structural Alloys for Nuclear Energy Applications**. Amsterdam: Elsevier, 2019. p. 163–210.

[13] SOUZA, E. S. **Caracterização de um sistema digital de aquisição de imagens radiográficas utilizando nêutrons térmicos e raios gama para inspeção de componentes mecânicos.** 123 p. Mestrado em Engenharia Mecânica — Universidade do Estado do Rio de Janeiro, Rio de Janeiro, 2012. 25 jul. de 2023. Avaiable at: <https://www.bdtd.uerj.br: 8443/handle/1/11699>.

[14] VOI, D. L. **Estudo da estrutura e da dinâmica moleculares da baquelite através de medidas de seções de choque para nêutrons.** 104 p. Doutorado em Ciências em Engenharia Nuclear e Planejamento Energético — Universidade Federal do Rio de Janeiro, Rio de Janeiro, 1990. 16 jun. de 2023. Avaiable at: <https://www.osti.gov/etdeweb/servlets/ purl/65440>.

[15] CUNHA, V. L. L. **Simulação do Reator Argonauta do IEN Utilizando o Código MCNPX.** 61 p. Mestrado em Engenharia Nuclear — Instituto Militar de Engenharia, Rio de Janeiro, 2010. Avaiable at: <http://https://inis.iaea.org/collection/NCLCollectionStore/_Public/49/072/49072011.pdf>.

[16] OLANDER, D.R.; **Fundamental Aspect of Nuclear Reactor Fuel Elements**. Springfield, United State Department of Commerce, 1976, p. 613.

[17] DUDERSTADT, J. J.; HAMILTON, L. J. **Nuclear Reactor Analysis**. 1. ed. New York: John Wiley and Sons, 1976. 650 p.